

PAPER • OPEN ACCESS

Morphological and Structural Changes in Microcrystalline Cellulose from OPEFB by Mechanical Grinding

To cite this article: T Herawan *et al* 2018 *IOP Conf. Ser.: Earth Environ. Sci.* **166** 012001

View the [article online](#) for updates and enhancements.

You may also like

- [Photomechanical modification of ZnS microcrystal to enhance electroluminescence by ultrashort-pulse laser processing](#)
Kyohei Nabesaka, Yasuaki Ishikawa, Yoichiro Hosokawa et al.
- [Characterization of Microcrystalline from Pineapple Leaf \(*Ananas comosus* L. Merr\)](#)
S Yuliasmi, Nerdy and A Husnita
- [Synthesis of microcrystalline cellulose from sugarcane bagasse and its incorporation into Polyvinyl Alcohol \(PVA\) matrix to test the composites mechanical properties](#)
Le Vinh Dien, Tran Tan Dat, Tran Thien Khanh et al.



ECS
The
Electrochemical
Society
Advancing solid state &
electrochemical science & technology

DISCOVER
how sustainability
intersects with
electrochemistry & solid
state science research

Morphological and Structural Changes in Microcrystalline Cellulose from OPEFB by Mechanical Grinding

T Herawan¹, F. R Panjaitan¹ and S Yamanaka²

¹Research Group for Palm Oil Product Development & Quality
Indonesian Oil Palm Research Institute, IOPRI,
Brigjen Katamso 51-Medan 20158, Indonesia

²College of Environmental Technology, Muroran Institute of Technology
Mizumoto-cho 27-1, Muroran 050-8585, Japan

E-mail: panjaitanf@yahoo.com

Abstract. Microcrystalline cellulose derived from oil palm empty fruit bunch (OPEFB) was grinded in planetary ball mill with dry state (without solvent) and solvent-assisted (ethanol and acetone). The effect of dry state and solvent-assisted on morphological and structural changes of microcrystalline cellulose were investigated. The structure changes, including particle size, powder morphology, crystalline structure, and molecular structure during the mechanical grinding were investigated by Laser Diffraction Particle Size Analyzer, SEM, XRD and FT-IR, respectively. The original fibrous microcrystalline cellulose was changed into irregular shape with finer micronized particles by dry state and solvent-assisted. SEM results showed that solvent-assisted significantly prevented the agglomeration phenomena during the grinding process, compared to dry state. The crystallinity after 4h solvent-assisted grinding showed fairly low crystallinity, while amorphous characteristic was observed with dry state grinding. The solvent-assisted led the hydrophilic parts of microcrystalline cellulose become stiff during the grinding that might be less deformed, leading to a fairly retain in crystallinity. The finer micronized particles were obtained under acetone-assisted and its crystallinity was fairly kept. XRD results indicated that crystalline form of origin microcrystalline was not changed by mechanical grinding.

1. Introduction

Cellulose is an attractive material for sustainable substitute synthetic polymer, because it is renewable, abundant resources, biodegradable, and relatively cheap. Recently, microcrystalline cellulose (MCC) from cellulosic material has been recognised for its diverse applications such as biomedical and pharmaceutical, foods, sensor and detector, construction, packaging, cosmetics, oil absorbents, aerogels, and other industries [1, 2]. Alpha cellulose from MCC is a partially depolymerized cellulose and is composed of crystalline and amorphous domain. MCC biomass conversion to transportation fuels, chemical platforms, and others functionalized-cellulose has attracted extensive attention. In all these synthesis, the catalytic depolymerisation of MCC to glucose is an important step from which transportation fuels, chemical platforms, and others functionalized-cellulose are then produced [3]. However, utilization of MCC has several limitations. It has highly-ordered and recalcitrant structure which is difficult to hydrolyse and insoluble in common solvents and thus restricting its efficient



applications. To improve the MCC reactivity towards catalytic depolymerisation prior to advance synthesis, physical pre-treatment-ball-milling is considered to be one of the facile techniques to its activation prior to the next process path [4]. Mechanical grinding, usually carried out by high-energy milling, refers to the use of friction, collision, impingement, shear or other mechanical actions to change the crystalline structure and physicochemical properties of solids [5]. Reduced the particle size, extent of specific surface area, amorphous cellulose, the crystalline structure is pre-requisite to make the MCC more accessible to degrading reagents. On these bases, the effect of dry state and solvent-assisted of mechanical grinding on morphological and structural of MCC was investigated. The significance of relate morphological and structural of MCC after grinding on transportation fuels, chemical platforms, and others functionalized-cellulose is our future research.

2. Material and Methods

2.1. Materials

α -Cellulose. α -Cellulose (raw material for OPEFB-MCC) was produced from oil palm empty fruit bunch (OPEFB). OPEFB cellulose has 88% of α -Cellulose content. The production of α -Cellulose was prepared from OPEFB by digested in sodium hydroxide to remove lignin and hemicellulose then bleached in sodium hypochlorite. Alkali hydrolysis was performed by soaking cellulose in sodium hydroxide for 12 hours. After soaking, cellulose was neutralized with water, dried and then ground to form powder cellulose. Detail methods described in the previous paper [6]. Acetone ($\geq 99.5\%$), ethanol (99.5%), sodium hydroxide and sodium hypochlorite were purchased from Merck, Indonesia.

2.2. Preparation of OPEFB-MCC

OPEFB-MCC was obtained from α -Cellulose-OPEFB, as described in [7]. The chemical used for soaking α -Cellulose-OPEFB was sodium hydroxide (NaOH) 4%. The obtained slurry was filtered and washed for several times with distilled water. The hydrolysis of soaked α -Cellulose-OPEFB was carried out with sulfuric acid (H_2SO_4) 6% for 2 h. At the end of hydrolysis process, the suspension (called as OPEFB-MCC) was centrifuged to remove the excessive acid solution and washed with distilled water. Finally, OPEFB-MCC oven dried at 60°C .

2.3. Mechanical grinding of OPEFB-MCC

OPEFB-MCC was ground in a planetary ball mill (Fritsch Pulverisette-7 premium line, Germany). The planetary ball mill was equipped with two zirconia pots of 80 cm^3 volume, each containing 80 g of yttria-stabilized zirconia milling beads (3 mm diameter) in close system. According to the manufacturer (Nikkato Corporation, Japan) the grinding media has a density of 5.950 kg m^{-3} and chemical composition of 95% of zirconia and 5% yttria. Mechanical grinding treatments adapting the method as described in [8] based on original procedures described in [9]. Solvent-assisted used were ethanol and acetone. Mechanical grinding operation was stopped for 15 min after every 1 h of grinding to prevent the inside of the milling pot from overheating. The conditions used are listed in **Table 1**.

Table 1. Mechanical grinding of OPEFB-MCC conditions

Process conditions	
Zirconia pot volume, V	80 cm^3
Mass of milling beads, W_B	80 g
Bead-filling ratio relative to the pot volume, J^a	0.28
Bead diameter	3 mm
OPEFB-MCC weight charge in the pot, W_s	4 g
Sample loading ratio to void fraction of the beads, U^b	0.28
Revolution speed	450 and 900 rpm
Grinding time	30 min; 4 h
Solvent-assisted weight charge (ethanol or acetone)	0.5 g

$$^a J = [W_B / \{\rho_{\text{ball}} \times (1 - 0.4)\}] / V$$

$$^b U = (W_s / \rho_p) / (0.4 \times J \times V)$$

2.4. Characterization

2.4.1. Particle size distribution determination

Particle size distribution of MCC was measured using a laser-diffraction analyser (MicroTrac MT3000EX, Nikkiso, Japan). All MCC samples were sonicated in an ultrasonic processor for 180 s before measuring.

2.4.2. Morphology

The morphology studies of the MCC were performed using a scanning electron microscope (SEM, JEOL JSM-6380A) with an acceleration voltage of 20 kV. Prior to analysis, the sample was covered a carbon film.

2.4.3. XRD analysis

Crystalline structures of MCC were investigated by using XRD on a Multi Flex-120 NP Rigaku (Japan) equipped with a Cu-K α anode ($\lambda = 1.5418 \text{ \AA}$), operated at a tension and current of 40 kV and 20 mA, respectively. Measurements were recorded at room temperature over the 2θ range $3\text{--}50^\circ$, with a 0.02° step size. The crystallinity and the crystallite size were calculated using previous method in [10].

2.4.4. Functional groups

Surface functional groups of MCC were determined from their infrared spectra analyzed by FTIR (JASCO FTIR-460 PlusK spectrometer). The spectrum was recorded in the range 4000 to 400 cm^{-1} at a resolution of 4 cm^{-1} and 32 scans.

3. Results and Discussion

3.1. Morphological Changes

XRD analysis was performed in order to evaluate structural changes undergone by MCC as a function of solvent-assisted and revolution speed of the mechanical grinding. XRD pattern of the initial OPEFB-MCC was shown in **Figure 1** (a) - (b). The crystalline structure was cellulose II showing its reflections around $2\theta = 12, 20$ and 22 [10,11]. After 4 h mechanical grinding course, the original fibrous MCC was converted into the aggregated globular particles resulting in decrease of the crystalline index (CrI). As shown in **Figure 1** (a), the grinding with dry state (4 h and 450 rpm) caused the characteristic shape of cellulose II crystal to completely lost (amorphous). The CrI of MCC under solvent-assisted with acetone or ethanol with low revolution speed (450 rpm) was fairly kept, but with higher revolution speed (900 rpm) it resulted some amorphous crystals. According to Gong et al (2010), the CrI was calculated, and the CrI values of acetone-assisted, ethanol assisted and dry state were ($20^\circ = 74.38\%$; $22^\circ = 64.39\%$), ($20^\circ = 55.68\%$; $22^\circ = 56.62\%$), and amorphous, respectively [10]. The initial state of CrI was ($20^\circ = 84.53\%$; $22^\circ = 82.97\%$). With further increase in revolution speed, 900 rpm, the crystal became amorphous in shorter time compared to revolution speed 450 rpm. These are attributed to the destruction of macromolecular chains and crystalline structure linked with ball impact and collision during the grinding course [12]. By increasing the milling speed improves the size reduction as shown in **Figure 1** (b). Milling speed seems to have positive effect on size reduction. It can be observed clearly that mechanical grinding caused decrease in peak intensity of MCC and broadening of diffraction peaks (**Figure 1** (a) and (b)). According to author in [13], the structures of MCC damaged during the grinding thus, resulting in the variation of morphologies such the increase of amorphous region ratio and hydrogen bond energy, and decrease crystallinity and crystalline size. The crystalline form of origin MCC was not changed by mechanical grinding.

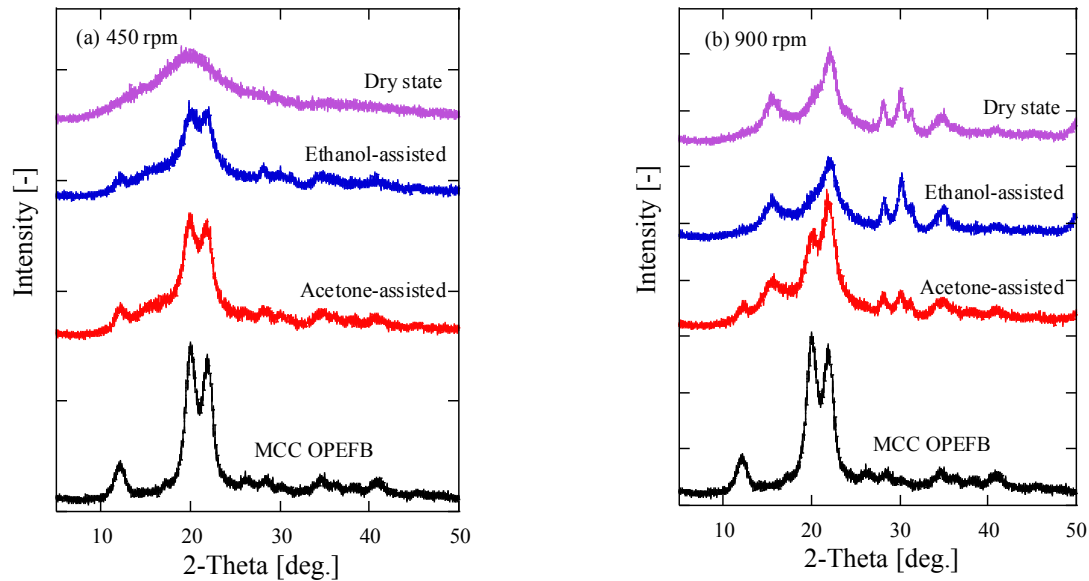
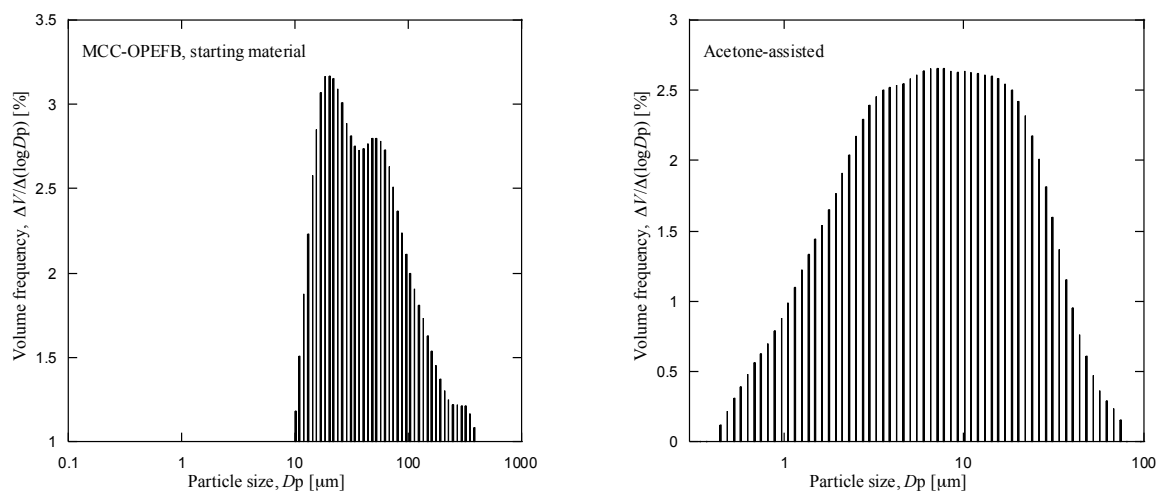


Figure 1. The XRD patterns (a) mechanical grinding with 450 rpm and 4 h; (b) 900 rpm and 30 min

3.2. Distribution of particle size

Mechanical grinding decreases particle size of MCC as results from impact, collision, friction and shear forces generated during the grinding course. This phenomenon changes the crystalline structure, induces the crystal defect and dislocation. At the same time, the grinding reduces the particle size and increases the specific surface area [4,8]. Using solvent-assisted method, coarse particles of MCC become finer (**Figure 2** and **3**). The D_{50} decreased from 435.38 μm to 6.54 μm , 7.51 μm , and 61.41 μm using acetone-assisted, ethanol-assisted and dry state methods at 450 rpm and 4 h, respectively. Increased in D_{50} was observed (**Figure 3**) when higher revolution speed of 900 rpm was applied. The D_{50} values are 11.27 μm , 21.148 μm , and 42.65 μm acetone-assisted, ethanol-assisted and dry state methods, respectively. This phenomenon was in agreement with Panjaitan et al (2016), by the SEM analysis, revealed agglomeration occurring during the grinding course [8]. The reason for distinguished D_{50} results on applying solvent-assisted was the interaction of solvents (ethanol or acetone) which partially coat the MCC during the grinding, thus prevents the agglomeration.



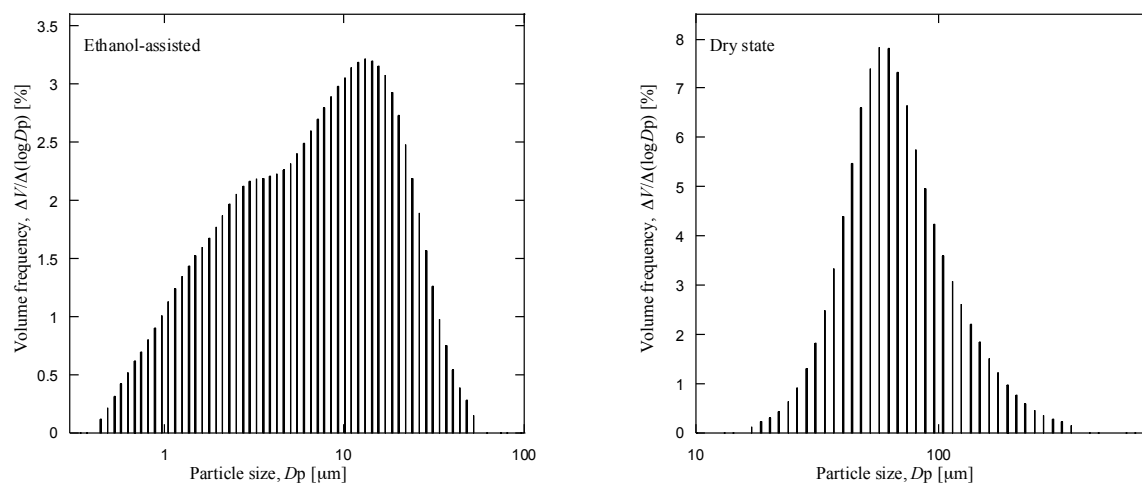


Figure 2. Distribution particle size of MCC at mechanical grinding with 450 rpm, 4 h

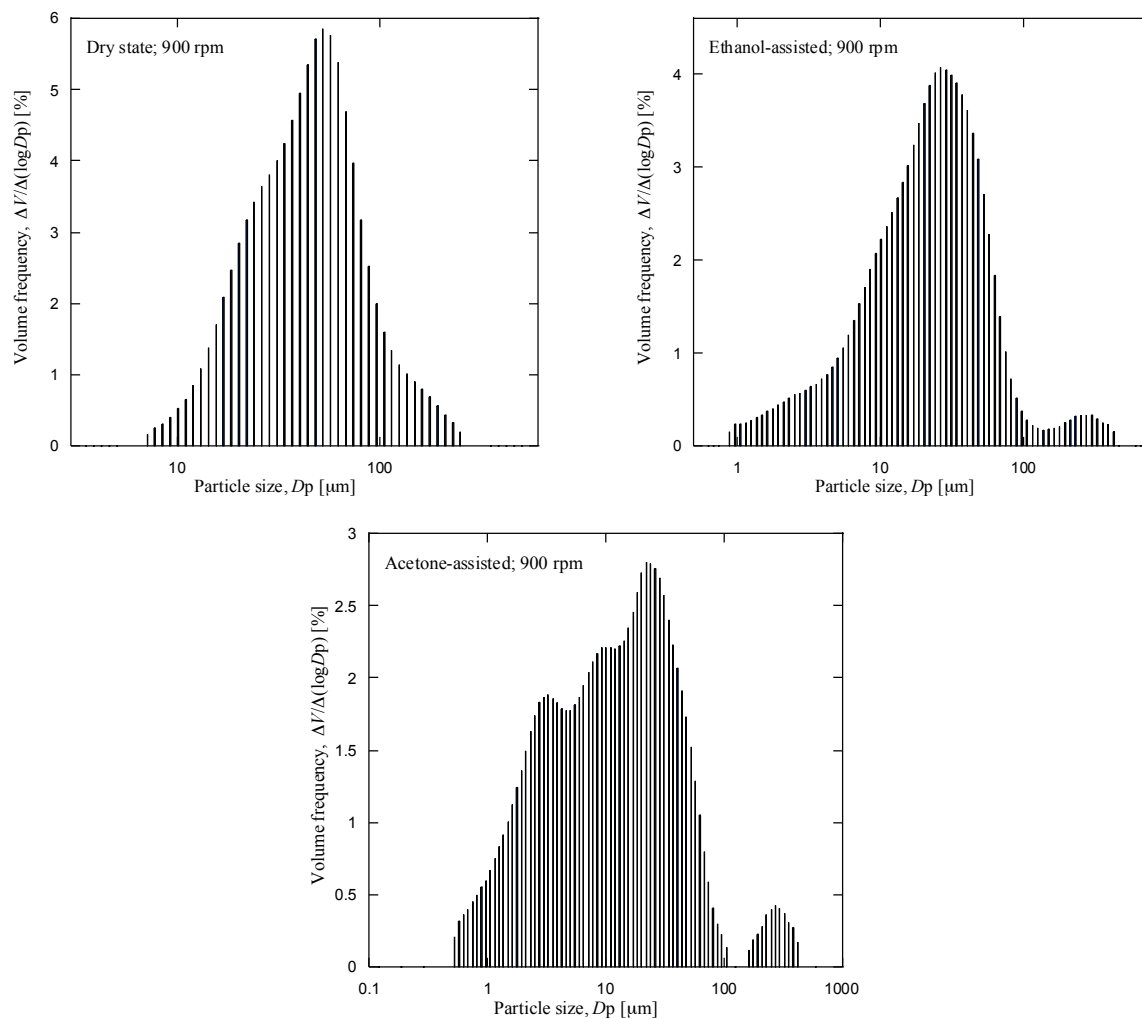


Figure 3. Distribution particle size of MCC at mechanical grinding with 900 rpm, 30 min

3.3. SEM Analysis

The morphologies of MCC after grinding course under different grinding conditions were shown in **Figure 4** and **5**. Mechanical grinding with solvent-assisted method generated better attrition and fracture in micronizing MCC compared to dry state method. Interaction of solvent during the grinding course is probably not only reacting with amorphous site of MCC leading to easier micronizing process but also coating the particles during the grinding course to prevent the agglomeration. Higher revolution speed (**Figure 5**) induced earlier agglomeration due to high collision frequency. In addition, it is possible that solvent coating concentration was not enough to reduce surface energy between the particles to prevent adhesiveness among the particles during the grinding course. The use of solvent-assisted and variation of revolution speed methods during the grinding course induced the transformation of crystalline cellulose of MCC. As a result, the MCC including crystalline, amorphous parts and their hydrophobic and hydrophilic planes [11] led the unique interaction between the MCC and solvent during the grinding course. Hydrophilic parts of MCC help the mobilization of solvent molecules to be adsorbed together with energy as a result of collision impact induced the cross-sectional cracks on MCC fibrous.

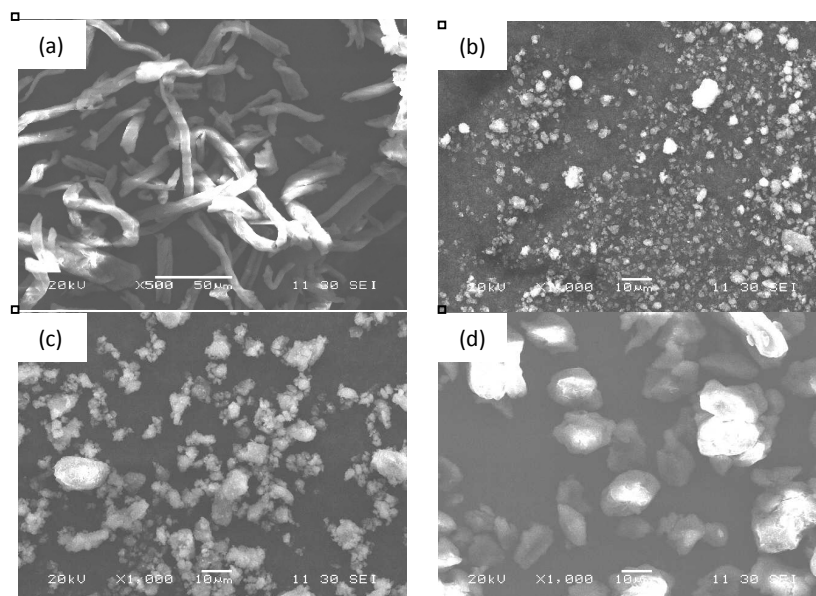


Figure 4. SEM analysis of MCC at mechanical grinding with 450 rpm, 4 h. (a) MCC OPEFB; (b) acetone-assisted; (c) ethanol-assisted; (d) dry state

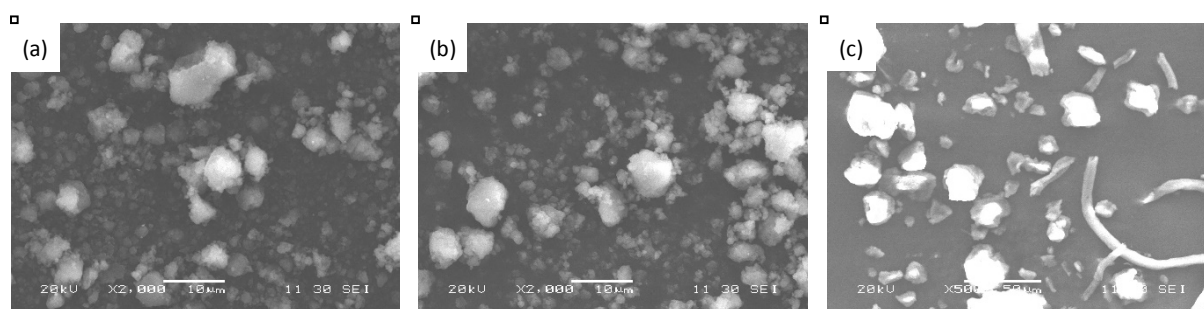


Figure 5. SEM analysis of MCC at mechanical grinding with 900 rpm, 30 min. (a) acetone-assisted; (b) ethanol-assisted; (c) dry state

3.4. FT-IR Analysis

In order to understand the changes of MCC molecular groups during the mechanical grinding, FT-IR analysis was carried out. **Figure 6** presents the FT-IR spectra before and after mechanical grinding

process. The difference spectra between the products and the original in the region O-H stretching from 3000 to 4000 cm^{-1} and C-O stretching vibrations from 800 to 1400 were compared among all products. The spectra in each region O-H stretching and C-O stretching was similar between the product with solvent-assisted and the original obtained. However, with dry state conditions, both in 450 and 900 rpm, each region O-H stretching and C-O stretching becomes wider in peak. According to XRD analysis (**Figure 1**), the crystals were amorphous. The O-H stretching bands of the products shifted toward lower wave numbers around 3350-3360 cm^{-1} . Possibly, during the grinding course, the MCC released free hydroxyl groups or ones weak hydrogen bonds causing the fracture in internal molecules of MCC [13].

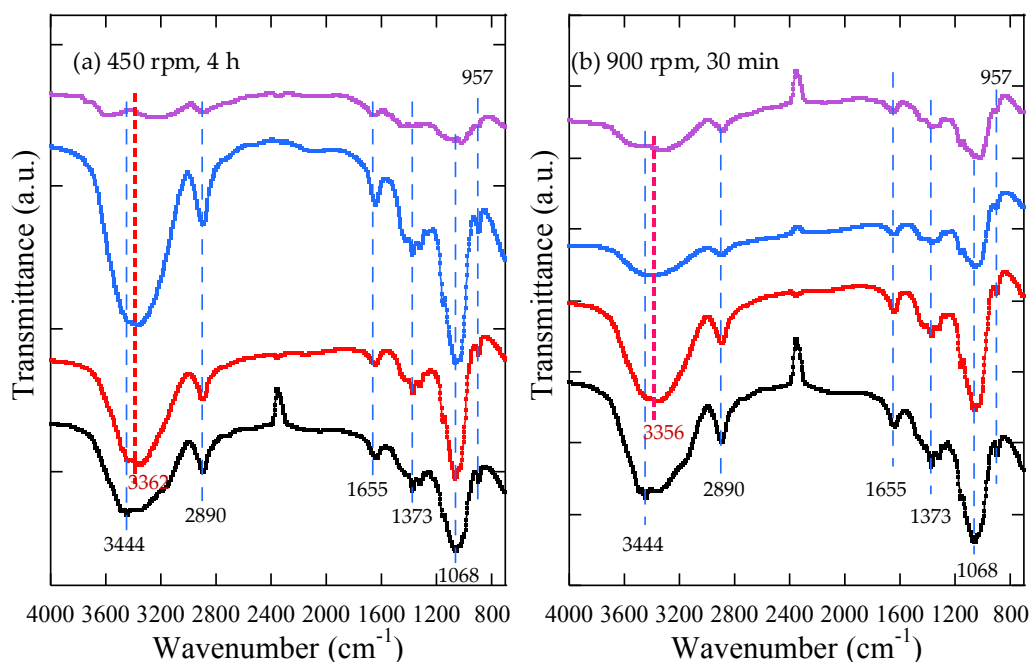


Figure 6. FT-IR spectra of MCC. (a) mechanical grinding with 450 rpm and 4 h; (b) 900 rpm and 30 min

4. Conclusion

The solvent-assisted method used in this work, i.e., acetone and ethanol affected the morphological and structural of MCC OPEFB under the mechanical grinding, giving the specific crystallinity, particle size distribution, and morphologies. The specific changes may be achieved by the solvent interaction and also the revolution speed of grinding process.

Acknowledgment

The authors would like to thank Oiso Takahiro and Yamanishi Tomoko in Surface and Chemical Engineering Lab., Muroran Institute of Technology, Hokkaido for their supporting in particle size distribution analyzing.

5. References

- [1] Korhonen Juuso T, Kettunen M, H A Ras Robin and Ikkala O 2011 *ACS Appl. Mater. Interfaces* **3** 1813
- [2] Haafiz M K Mohamad, Hassan A, Zakaria Z and Inuwa I M 2014 *Carbohydrate Polymers* **103** 119
- [3] Zhang Q, Benoit M, De Oliveira Vigier K, Barrault J, Jegou G, Philippe M and Jerome F 2013

- Green Chem.* **15** 963
- [4] Yuan X, Liu S, Feng G, Liu Y, Li Y, Lu H and Liang B 2016 *Korean Journal of Chemical Engineering* **33** 2134
- [5] Ago M, Endo T and Hirotsu T 2004 *Cellulose* **11** 163
- [6] Herawan T and Rivani M 2015 *Advanced Materials Research* **1123** 173
- [7] Herawan T and Rivani M 2013 *J. Pen. Kelapa Sawit* **21** 31
- [8] Panjaitan F R, Yamanaka S and Kuga Y 2016 *Advanced Powder Technology* **28** 1627
- [9] Yamanaka S, Suzuma A, Fujimoto T and Kuga Y 2013 *J. of Nanoparticle Research* **1573** 1
- [10] Gong J, Li J, Xu J, Xiang Z and Mo L 2017 *RSC Adv.* **7** 33486
- [11] Ago M, T. Endo and K. Okajima, 2007 *Polymer Journal* **39**(5) 435
- [12] Huang Z, Liang X, Hu H, Gao L, Chen Y and Tong Z, 2009 *Polym Degrad Stab* **94** 1737
- [13] Hu, H, Y Zhang, X Liu, Z Huang, Y Chen, M Yang, X Qin and Z Feng, 2014 *Polym. Bull* **71** 453